

INSTANTSWAP: Fast Customized Concept Swapping across Sharp Shape Differences

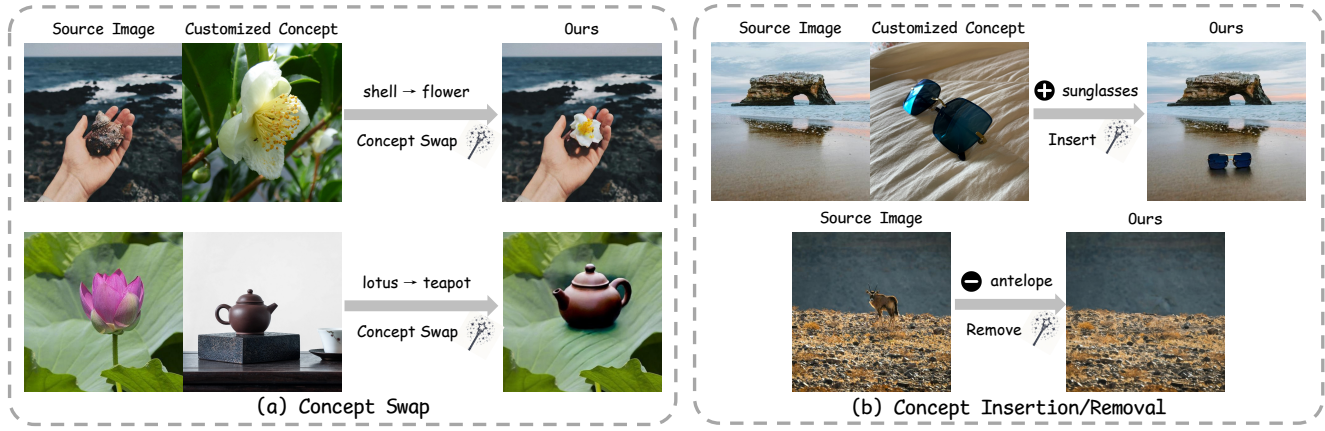
Chenyang Zhu^{1,*}Kai Li^{2,*†}Yue Ma^{3,*}Longxiang Tang¹Chengyu Fang¹Chubin Chen¹Qifeng Chen³Xiu Li^{1,†}¹ Tsinghua University² Meta Reality Labs³ HKUST<https://instantswap.github.io/>

Fig 1. Visual results of INSTANTSWAP. Our approach can seamlessly swap a source concept with a customized concept in an image, even with great shape differences. Moreover, INSTANTSWAP can be used for other tasks, such as concept insertion and removal.

Abstract

Recent advances in Customized Concept Swapping (CCS) enable a text-to-image model to swap a concept in the source image with a customized target concept. However, the existing methods still face the challenges of **inconsistency** and **inefficiency**. They struggle to maintain consistency in both the foreground and background during concept swapping, especially when the shape difference is large between objects. Additionally, they either require time-consuming training processes or involve redundant calculations during inference. To tackle these issues, we introduce INSTANTSWAP, a new CCS method that aims to handle sharp shape disparity at speed. Specifically, we first extract the bbox of the object in the source image automatically based on attention map analysis and leverage the bbox to achieve both foreground and background consistency. For background consistency, we remove the gradient outside the bbox during the swapping process so that the background is free from being modified. For foreground

consistency, we employ a cross-attention mechanism to inject semantic information into both source and target concepts inside the box. This helps learn semantic-enhanced representations that encourage the swapping process to focus on the foreground objects. To improve swapping speed, we avoid computing gradients at each timestep but instead calculate them periodically to reduce the number of forward passes, which improves efficiency a lot with a little sacrifice on performance. Finally, we establish a benchmark dataset to facilitate comprehensive evaluation. Extensive evaluations demonstrate the superiority and versatility of INSTANTSWAP.

1. Introduction

We explore the task of Customized Concept Swapping (CCS), a subtask of text-to-image (T2I) generation, which aims to replace a concept in a source image with a highly customized new concept. Combined with diffusion models [7, 38, 43], recent CCS methods demonstrate widespread applicability in areas such as selfie enhance-

* Equal contribution.

† Corresponding Authors.



Fig 2. Our INSTANTSWAP achieves better swapping consistency than the existing methods.

ment, photo blog creation, and comic creation.

Early work [49] in CCS primarily relies on copy-paste techniques, which are rough and unreliable. By integrating powerful customization techniques [26, 44] with image editing methods [18, 19], a series of works [4, 13, 14, 28] have been proposed. Although achieving remarkable success, these approaches still face the problems of *inconsistency* and *inefficiency* as shown in Fig. 2. (1) *Inconsistency*: Attention-based methods such as PhotoSwap [13] and P2P [18] maintain background consistency well but struggle with shape differences between source and target concepts, resulting in foreground inconsistency. Score distillation based methods such as SDS [39], DDS [19], and CDS [36] fail to generate foreground concepts precisely and alter the background significantly, causing both foreground and background inconsistency. (2) *Inefficiency*: Attention-based methods require an inefficient training phase [24, 35] on source image to maintain background consistency. While score distillation based methods are training-free, they still require redundant calculations of forward passes at each timestep, leading to inference inefficiency.

To address the aforementioned issues, we propose INSTANTSWAP, a training-free framework that *efficiently* performs customized concept swapping across shape differences while maintaining **both foreground and background consistency**. Specifically, we extract the bounding box (bbox) that indicates the position of the source concept from the enhanced cross-attention map of the source image. With this bbox, we perform the background gradient masking (BGM) strategy to prevent modifications outside the bbox, thus ensuring background consistency. Moreover, to improve foreground consistency, we leverage the semantic information to highlight the cross-attention maps of source and target concepts respectively within the bbox. This strategy leads to the semantic-enhanced concept representation (SECR), which facilitates precise foreground swapping. Finally, we introduce the Step-skipping Gradient Updating (SSGU) strategy, which only performs forward passes at certain timesteps to calculate gradients. For the timesteps without direct gradient computations, we reuse the previously obtained gradients for updates. Through this strategy, we reduce the total number of forward passes and improve the efficiency of our method.

Since the CCS is a recently proposed task, no dedicated evaluation benchmark currently exists. To address this gap, we introduce *ConSwapBench*, the first benchmark dataset specifically designed for CCS. *ConSwapBench* comprises two sub-benchmarks: ConceptBench and SwapBench. ConceptBench contains images representing target concepts, while SwapBench includes images with one or more concepts to be swapped, serving as source images.

Through extensive qualitative and quantitative comparisons, we demonstrate the effectiveness and superiority of our INSTANTSWAP. We also conduct comprehensive ablation studies to verify the effectiveness of each component of our approach. Additionally, we further extend our INSTANTSWAP to related tasks, proving its efficacy and versatility. Our contributions are summarized as follows:

- We propose INSTANTSWAP, a novel training-free customized concept swapping (CCS) framework, which enables efficient concept swapping across sharp shape differences.
- We design the background gradient masking (BGM) strategy and semantic-enhanced concept representation (SECR) to improve the background and foreground consistency respectively. Moreover, we adopt a step-skipping gradient updating (SSGU) strategy to reduce redundant computation and improve efficiency.
- To provide a comprehensive evaluation for CCS, we introduce *ConSwapBench*, the first benchmark for customized concept swapping. Extensive qualitative and quantitative evaluations demonstrate the effectiveness and superiority of our INSTANTSWAP.

2. Related work

2.1. Diffusion-based Image Editing

Image Editing is a fundamental and popular topic in computer vision. Previous works based on Generative Adversarial Networks (GAN) [12] only focus on specific object domains, which limits the application. With the emergence of diffusion model [43], image editing is now able to modify various objects through prompts. These methods are mainly divided into five categories: instruction-based methods, blending-based, attention-based, inversion-based,

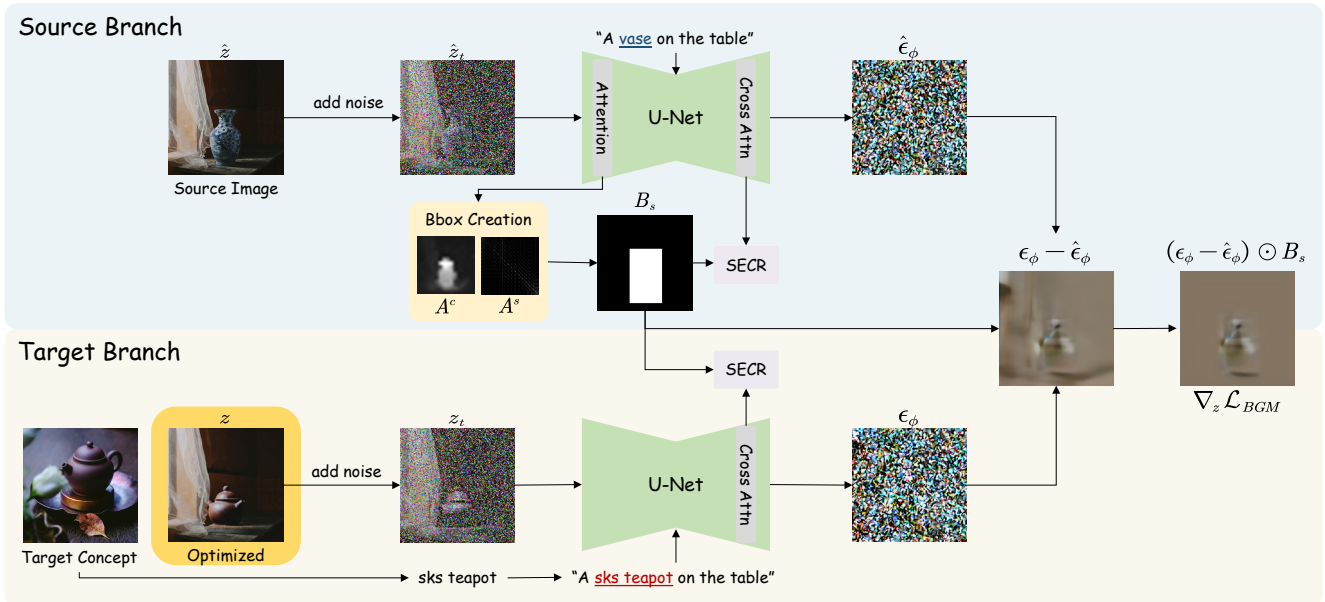


Fig 3. Overall pipeline of INSTANTSWAP. We first obtain the bbox of the source concept automatically. The obtained bbox is input into SECR in both the source and target branches to enhance the foreground swapping consistency. Additionally, the source and target branches generate the prediction of noise for the source and target images based on their respective prompts. The predicted noise, along with the bbox, is used for the BGM to preserve background consistency.

and score distillation based methods. Instruction-based methods [1, 11, 23, 31, 50] typically require an instruction editing dataset to train the diffusion model. Blending-based methods [6, 22, 27, 52] merge the source and target prompts to guide the editing process, while attention-based methods [2, 15, 18, 46] inject the attention feature of the source image. Both methods have lower editing costs but poorer background preservation and prompt alignment. Inversion-based methods [8, 24, 32, 34, 35] aim to reverse the fixed trajectory generated by the forward pass to reproduce the source image. These methods can serve as an extra training phase to enhance the background consistency of attention-based methods. Finally, score distillation based methods [3, 19, 25, 30, 33, 36] draw on the optimization process of SDS [39], using score distillation-based loss to optimize the source image for editing. These methods are more flexible than the previous ones but still face challenges with background preservation.

2.2. Concept Swapping

Concept swapping, a subtask of general image editing, focuses on replacing the source concept in an image with a user-specified target concept. This task is first proposed by PbE [49], which employs a CLIP encoder to extract features of the target concept and inject them into the UNet through a cross-attention layer. After that, concurrent works [4, 13, 28, 47] extend concept swapping into the customization field [10, 54]. They combine attention-based

editing methods [18, 46], with tuning-based customization methods [26, 44] to achieve customized concept swapping. Building on Photoswap, SwapAnything [14] further obtains masks with external modules to specify the locations of objects in the source image. We improved the existing method in three key aspects. Firstly, we employ bounding boxes instead of masks as spatial indicators of the source concept, allowing greater flexibility for shape variation during concept swapping. Secondly, we use bounding boxes to prevent background changes via gradient masking, thus ensuring background consistency. Third, we augment concept representation with semantic information to maintain foreground consistency. Finally, rather than executing forward passes at every timestep, we execute them only at specific intervals to enhance efficiency.

3. Method

Given a set of images, $\mathcal{X}_t = \{x_i\}_{i=1}^M$ representing a specific concept O_t , along with an image x_s and a prompt p_s describing a source concept O_s , the objective of CCS is to “seamlessly” replace O_s in x_s with O_t according to a target prompt P_t , resulting in a final target image x_t . An ideal customized concept swapping should handle the shape differences between source and target concepts to preserve swapping consistency while maintaining satisfactory efficiency. We introduce INSTANTSWAP to achieve this. INSTANTSWAP is based on Stable Diffusion and extends from the score distillation based image editing methods [19, 39].

3.1. Preliminaries

3.1.1 Stable Diffusion

In this paper, the foundational model utilized for text-to-image generation is Stable Diffusion [43]. It takes a text prompt P as input and generates the corresponding image x . Stable Diffusion consists of three main components: an autoencoder $(\mathcal{E}(\cdot), \mathcal{D}(\cdot))$, a CLIP text encoder $\tau(\cdot)$ and a U-Net $\epsilon_\phi(\cdot)$. Typically, it is trained with the guidance of the following reconstruction loss:

$$\mathcal{L}_{rec} = \mathbb{E}_{z, \epsilon \sim \mathcal{N}(0, 1), t, P} [\|\epsilon - \epsilon_\phi(z_t, t, \tau(P))\|_2^2], \quad (1)$$

where $\epsilon \sim \mathcal{N}(0, 1)$ is a randomly sampled noise, t denotes the time step. The calculation of z_t is given by $z_t = \alpha_t z + \sigma_t \epsilon$, where the coefficients α_t and σ_t are provided by the noise scheduler.

3.1.2 Score Distillation Based Image Editing

Different from traditional attention-based image editing, score distillation based methods achieve image editing through iterative optimization with a score distillation loss. Given the latent feature z of source image and a denoising U-Net $\epsilon_\phi(\cdot)$, SDS [39] can optimize the latent feature z of the image to align with the target prompt P_t by employing the following loss:

$$\mathcal{L}_{SDS} = \|\epsilon_\phi(z_t, t, \tau(P_t)) - \epsilon\|_2^2, \quad (2)$$

where ϵ and t are randomly sampled noise and timestep.

The resulting image SDS is very blurry and only contains foreground objects in the target prompt P_t . To address this issue, DDS [19] expresses the gradient of Eq. (2) as

$$\nabla_z \mathcal{L}_{SDS}(z_t, t, \tau(P_t)) = \delta_{tgt} + \delta_{bias}, \quad (3)$$

where δ_{tgt} indicates the direction aligned with the target prompt and δ_{bias} refers to undesired part that makes the image blurry. Based on this, DDS further utilizes the fixed latent \hat{z}_t of the source image and the source prompt P_s to approximate the bias component in Eq. (3):

$$\nabla_z \mathcal{L}_{SDS}(\hat{z}_t, t, \tau(P_s)) \approx \hat{\delta}_{bias} \approx \delta_{bias}. \quad (4)$$

Finally, DDS is represented by the difference of Eq. (3) and Eq. (4):

$$\begin{aligned} \nabla_z \mathcal{L}_{DDS} &= \nabla_z \mathcal{L}_{SDS}(z_t, t, \tau(P_t)) \\ &\quad - \nabla_z \mathcal{L}_{SDS}(\hat{z}_t, t, \tau(P_s)) \\ &\approx \delta_{tgt}. \end{aligned} \quad (5)$$

Based on Eq. (5), the loss of DDS is given by

$$\mathcal{L}_{DDS} = \|\epsilon_\phi(z_t, t, \tau(P_t)) - \hat{\epsilon}_\phi(\hat{z}_t, t, \tau(P_s))\|_2^2. \quad (6)$$

3.2. INSTANTSWAP

Directly extending score distillation based editing methods to the task of CCS encounters the challenge of inconsistency. These methods optimize the background and foreground simultaneously, causing cross-interference and leading to undesirable inconsistency. To address these limitations, we first propose a strategy to *automatically* locate objects to be edited, resulting in the object bounding box (bbox). With this bbox, we propose a background gradient masking technique to remove gradients in the background region and confine swapping to the foreground region. To further enhance foreground swapping consistency, we propose to learn Semantic-enhanced concept representations for both source and target concepts based on an attention map feature injection mechanism. An overview of our method is presented in Fig. 3.

3.2.1 Automatic Bounding Box Generation

We first automatically obtain the bbox to indicate the position of the concept O_s in the source image. Given the source image x_s and the source prompt P_s , we perform a forward pass with the U-Net $\epsilon_\phi(\cdot)$ and obtain the cross-attention map A^c and self-attention map A^s through:

$$A = \text{Softmax} \left(\frac{QK^T}{\sqrt{d'}} \right) V, \quad (7)$$

where Q is the query vector projected from the image features, d' represents the output dimension of key and query features. K is the key vector and V is the value vector. For cross-attention maps A^c , K and V are projected from the text embeddings $\tau(P)$. For self-attention maps A^s , K , and V are projected from the image features. Directly applying a threshold on the A^c can yield a coarse-grained mask, which cannot accurately reflect the location of O_s . Inspired by [37, 53], we modify the A^c as follows:

$$\hat{A}^c = A^s \cdot (A^c)^\alpha. \quad (8)$$

Based on Eq. (7), all values in A^c range between 0 and 1. Therefore, element-wise exponentiation of A^c by α can weaken the activation of non-target regions. Additionally, as mentioned in [29], A^s contains rich structural information. This information can effectively assist \hat{A}^c in better activating the target regions. Finally, we apply the threshold β to \hat{A}^c to obtain the mask. Subsequently, we converted the mask into the bbox B_s based on the minimum and maximum coordinates of all foreground points within the mask. This strategy allows us to obtain the bbox B_s without any additional modules. We intentionally set a relatively loose constraint on the mask to obtain a bbox that completely covers the source concept. We discuss the effectiveness of our automatically obtained bboxes in Sec. 4.5.

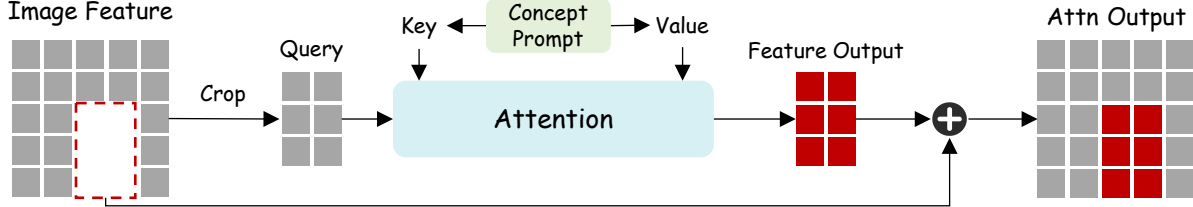


Fig 4. Overview of SECR.

3.2.2 Background Gradient Masking

With the object bbox, we propose a background gradient masking (BGM) approach to ensure that the concept swap is confined to the foreground region. Given the latent feature \hat{z} of the source image and the latent feature z of the target image, where z is initialized to \hat{z} and is continuously optimized to obtain the final target image x_t . Based on Eq. (6), we first obtain the gradient of z :

$$\nabla_z \mathcal{L} = (\epsilon_\phi(z_t, t, \tau(P_t)) - \hat{\epsilon}_\phi(\hat{z}_t, t, \tau(P_s))) \frac{\partial \epsilon_\phi(z_t, t, \tau(P_t))}{\partial z_t} \frac{\partial z_t}{\partial z}. \quad (9)$$

As stated in [39], the mid term is a U-Net Jacobian term and can be omitted, and $\alpha_t = \partial z_t / \partial z$ is a constant which can be represented as $w(t)$:

$$\nabla_z \mathcal{L} = w(t)(\epsilon_\phi(z_t, t, \tau(P_t)) - \hat{\epsilon}_\phi(\hat{z}_t, t, \tau(P_s))). \quad (10)$$

This gradient shares the same dimension as z , which means it can update z in a pixel-wise manner. However, this will update the foreground and background simultaneously, producing inconsistent background. To remedy this, we apply the bbox B_s on Eq. (10) to mask the gradients related to the background before back propagation and obtain our BGM:

$$\nabla_z \mathcal{L}_{BGM} = w(t)(\epsilon_\phi(z_t, t, \tau(P_t)) - \hat{\epsilon}_\phi(\hat{z}_t, t, \tau(P_s))) \odot B_s. \quad (11)$$

This simple masking strategy prevents the background from being updated and thus ensures background consistency.

3.2.3 Semantic-enhanced Concept Representation

The BGM module maintains the background consistency during swapping. However, whether the source concept can be replaced with the target concept cannot be guaranteed. This limitation arises because the optimization of Eq. (11) is still carried out at the entire feature map level of both the source latent \hat{z}_t and target latent z_t without distinguishing between the foreground and the background. To address this, we propose to obtain Semantic-enhanced concept representations for both source and target concepts and emphasize their locations within the foreground region during concept swapping.

Let F_s be the source image feature and p_s represent the prompt of source concept (e.g. “rose”), the semantic embedding c_s can be acquired through $c_s = \tau(p_s)$. We first resize the previously obtained object bbox to fit the dimensions of the source image feature F_s , resulting in the feature bbox B_f . We then crop F_s with B_f to get a regional image feature f_s . With f_s , we calculate the query vector through $Q_s = W^q \cdot f_s$. After that, we can obtain the key and value vectors through:

$$K_s = W^k \cdot c_s, V_s = W^v \cdot c_s. \quad (12)$$

Then the final partial attention output is calculated as follows:

$$\hat{f}_s = \text{Softmax} \left(\frac{Q_s K_s^T}{\sqrt{d'}} \right) V_s, \quad (13)$$

where d' represents the output dimension of key and query features. In this way, we inject the semantic information of the source concept into the cross-attention map, resulting in regional concept representation \hat{f}_s . We then map \hat{f}_s back to the original feature map F_s to get a Semantic-enhanced representation \hat{F}_s for the entire source image. Fig. 4 illustrates the process. In the target branch, we first convert the target concept into semantic space with DreamBooth, using a specific rare token (e.g., “sks”) to represent the concept. With the target prompt p_t (e.g., “sks teapot”) and the feature bbox B_f , we similarly apply this process for the target image feature F_t and obtain the semantic-enhanced representation \hat{F}_t for the target image.

Through proactive injection of semantic guidance, we provide the source and target branches with Semantic-enhanced concept representation within the foreground region. Consequently, SECR transforms the target branch into a target concept adder and the source branch into a source concept remover. Their collaboration results in precise and seamless concept swapping, thus enhancing the foreground consistency. Moreover, SECR can also facilitate concept insertion and removal, which is further discussed in Sec. 4.6.

3.2.4 Step-skipping Gradient Updating

After addressing the problem of inconsistency, we turn our attention to the challenge of inefficiency. As illustrated in Fig. 5, previous methods calculate the gradient at each

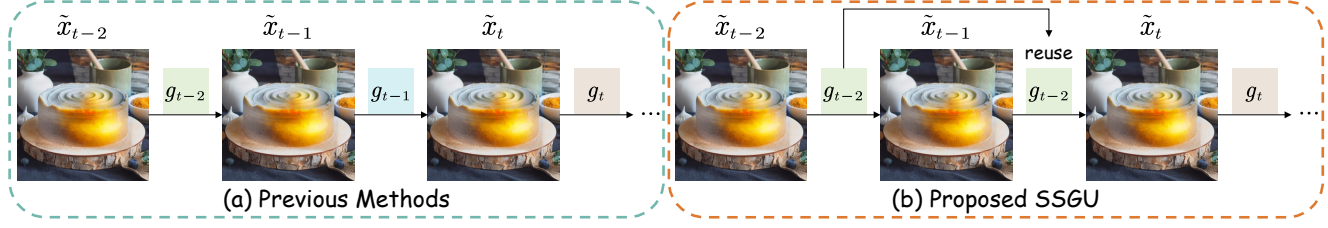


Fig 5. Comparison between our SSGU and previous methods.

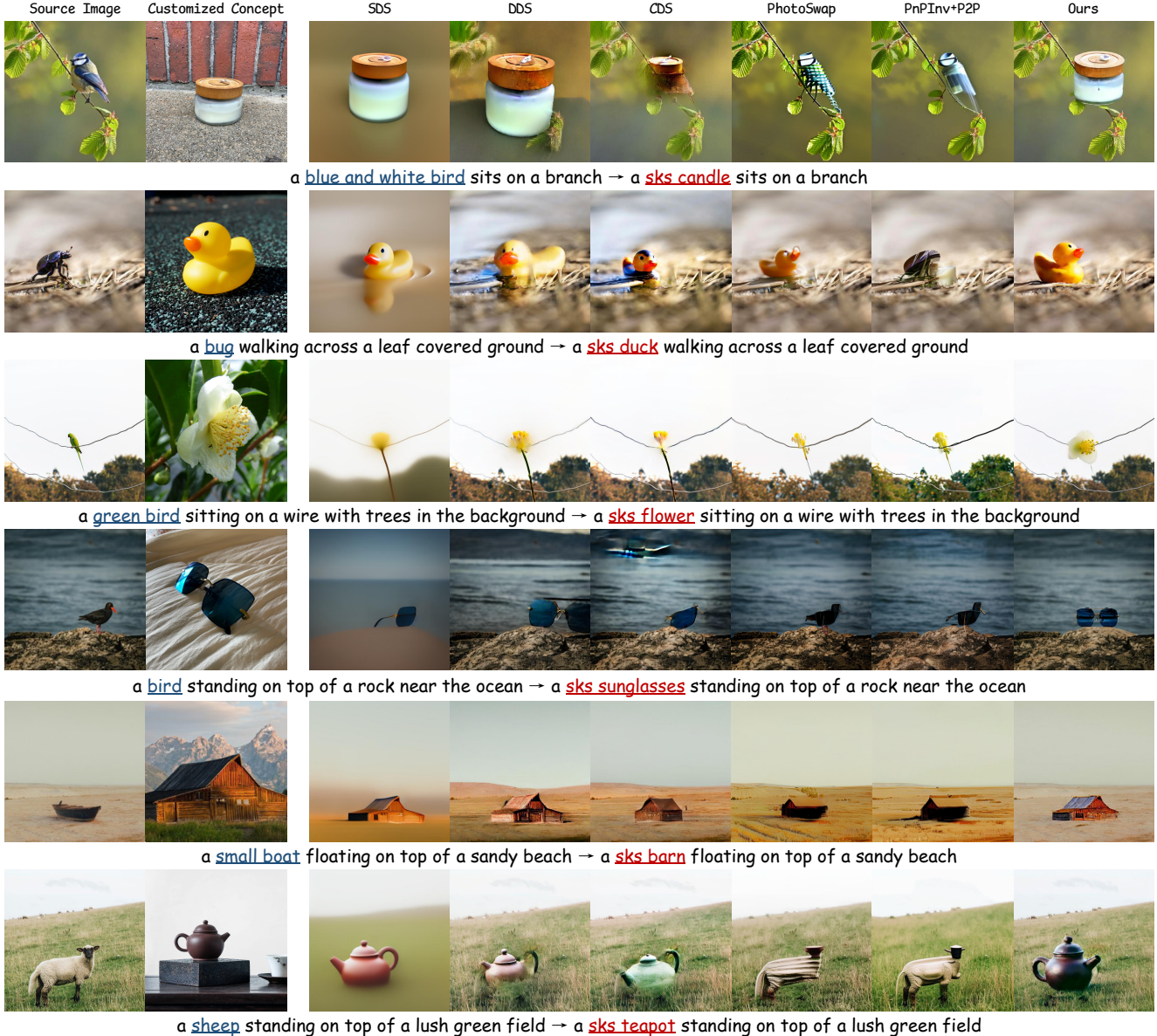


Fig 6. Qualitative comparisons between our INSTANTSWAP and other methods. More qualitative results as well as the used bboxes can be found in *Supp.*

timestep. However, the success of DDIM [45] in accelerating DDPM [21] motivates us to consider: *Can we skip the calculation of gradients at certain timesteps?* Dur-

ing concept swapping, we observe that the effect of gradient updates on the target image is similar across adjacent timesteps (see detailed results in *Supp.*). Based on this ob-

Table 1. Quantitative comparisons. Our method outperforms all the compared methods in all the selected metrics. **Red** stands for the best result, **Blue** stands for the second best result.

Method	FG		BG			Overall	
	CLIP-I \uparrow	PSNR \uparrow	LPIPS $\times 10^3 \downarrow$	MSE $\times 10^4 \downarrow$	SSIM $\times 10^2 \uparrow$	CLIP-T \uparrow	Time (s) \downarrow
SDS	73.70	20.79	339.51	107.53	72.59	23.53	40.37
DDS	71.05	24.07	89.80	53.08	83.44	23.99	66.89
CDS	71.69	23.36	90.35	63.41	83.21	24.17	140.26
PhotoSwap	70.15	24.24	120.62	56.64	80.56	22.38	140.34
PnPInv+P2P	70.74	24.63	108.22	47.49	82.07	24.25	37.02
Ours	75.00	27.39	47.68	27.87	86.58	25.74	19.83

servation, we propose the step-skipping Gradient Updating (SSGU) strategy. The key insight of SSGU is that *skipping some gradient calculations does not significantly sacrifice the swapping consistency while considerably improving efficiency*. As a result, our SSGU calculates gradients at interval timesteps and reuses the previously calculated gradients during the intervening timesteps.

We define our entire pipeline as \mathcal{F} , given the source image x_s , the timestep t , and the intermediate target image \tilde{x}_t at timestep t . We can obtain the gradient g_t and the output intermediate target image \tilde{x}_{t+1} at timestep t as follows:

$$g_t = \mathcal{F}(x_s, \tilde{x}_t, t), \quad (14)$$

$$\tilde{x}_{t+1} = \tilde{x}_t - \eta g_t, \quad (15)$$

where η is the learning rate. Our SSGU periodically retains some anchor gradients and skips the forward passes between two anchor gradients. The step-skipping period is controlled by the SSGU factor λ . The set of anchor gradients can be defined as:

$$\mathbb{G} = \{g_{\lambda k}\}, k = 0, 1 \dots, [T/\lambda], \quad (16)$$

where T is the ended timestep. For any intervening timestep t , we use its nearest former anchor gradient to update the intermediate target image \tilde{x}_t . Taking $\lambda = 2$ as an example, we assume that t is an even number and $g_{t-2}, g_t \in \mathbb{G}$. SSGU updates \tilde{x}_{t-2} and \tilde{x}_{t-1} with the anchor gradient g_{t-2} :

$$g_{t-2} = \mathcal{F}(x_s, \tilde{x}_{t-2}, t-2), \quad (17)$$

$$\tilde{x}_{t-1} = \tilde{x}_{t-2} - \eta g_{t-2}, \quad (18)$$

$$\tilde{x}_t = \tilde{x}_{t-1} - \eta g_{t-2}. \quad (19)$$

For the next timestep t , another anchor gradient g_t is used to update x_t . As a result, our SSGU reduces the number of forward passes during the entire concept swapping process to $1/\lambda$ of the original count. Since the forward pass accounts for approximately 95% of the total inference time (see detailed analysis in *Supp.*), our SSGU can improve the overall inference speed of our method by approximately λ times,

with minimal effect on swapping consistency (see Sec. 4.5). Furthermore, our SSGU can be transferred to other score distillation based methods to improve their efficiency in the same way, which is further discussed in Sec. 4.6.

4. Experiments

4.1. Implementation Details

We conduct the experiments with Stable Diffusion [43] v2.1-base on a single RTX3090. We use the customized checkpoint from DreamBooth [44] to introduce concepts. We set the SSGU factor λ to 5, α to 2, β to 0.5 and the guidance scale to 7.5. The bbox is obtained through the first three steps. Subsequently, we use SGD [42] with a learning rate of 0.1 to optimize for 550 steps of iterations.

4.2. ConSwapBench

Despite the significant application potential of customized concept swapping, there is currently no dedicated evaluation benchmark. To meet the needs of comprehensive evaluation, we introduce *ConSwapBench*, the first benchmark dataset specifically designed for customized concept swapping. *ConSwapBench* consists of two sub-benchmarks: ConceptBench and SwapBench. ConceptBench comprises 62 images covering 10 different target concepts used for customization, while SwapBench includes 160 real images containing one or more objects to be swapped, serving as source images. For each image in SwapBench, we use Grounding SAM [41] to acquire the bbox of the foreground concepts as the ground truth for evaluation purposes. We apply each customized concept from ConceptBench to perform concept swaps on each image in SwapBench, ultimately generating a total of 1,600 images for evaluation. More details can be found in *Supp.*

4.3. Qualitative Comparison

Since customized concept swapping is a relatively novel task, there are limited methods available for direct comparison. Consequently, we include SOTA image editing



Fig 7. Qualitative results of the ablation study on: *Left*: BGM and SECR. *Right*: different bboxes.

methods and adapt them for customized concept swapping. We include the following methods: (1) *Score distillation based* methods: SDS [39], DDS [19], and CDS [36]; (2) *Attention-based* methods: PhotoSwap [13], PnPInv [24], and P2P [18]. We excluded SwapAnything [14] as it is not publicly available. The qualitative results are illustrated in Fig. 6. We find that score distillation based methods can accommodate shape variations during concept swapping. However, they exhibit poor foreground fidelity (3rd and 6th rows) and lead to unnecessary modifications on the background (1st and 2nd rows). Attention-based methods are unable to manage shape variations (4th row) and also struggle with maintaining background consistency (5th row). In contrast, our method demonstrates superior performance in addressing shape variations and maintaining swapping consistency.

4.4. Quantitative Comparison

We also conduct a thorough quantitative comparison on *ConSwapBench*. For each generated image, we first use the ground truth bbox in SwapBench to obtain their foreground and background respectively. We use seven different metrics to evaluate the methods from three aspects: (1) Foreground consistency: We calculate the CLIP Image Score [40] between the foreground of generated images and the images of customized concepts. (2) Background consistency: We use the four metrics, PSNR, LPIPS [51], MSE, SSIM [48] to evaluate the background consistency. (3) Overall consistency and efficiency: We calculate the CLIP Text Score [20] between generated images and target prompts to evaluate the overall prompt consistency. We also report the inference time of each method to evaluate their efficiency. As shown in Tab. 1, our method outperforms other methods on all seven metrics.

4.5. Ablation Study

BGM. To verify the effectiveness of BGM in background preservation, we conduct an ablation study by removing

BGM. As illustrated in the second column of Fig. 7, while our method can still achieve concept swapping without BGM, it causes serious modifications on the background. In contrast, our full method not only maintains high foreground fidelity but also effectively preserves the background consistency. We further conduct a quantitative analysis of the background consistency and prompt consistency, as shown in Tab. 2. Our full method outperforms in all metrics.

Table 2. Quantitative ablation results of BGM.

Method	PSNR ↑	LPIPS ↓	MSE ↓	SSIM ↑	CLIP-T ↑
w/o BGM	18.03	249.24	184.19	72.25	23.08
Ours	27.39	47.68	27.87	86.58	25.74

Automatic bounding box detection mechanism. We further verify the effectiveness of our boxes by using ground truth (GT) bboxes from SwapBench to replace the automatically obtained bboxes. As shown in Fig. 7, although GT bboxes accurately indicate the location of the source concept, they prevent our method from fully swapping the source concept. Compared to GT bboxes, our bboxes are relatively larger and can fully cover the source concept, thereby facilitating complete concept swapping. We also provide quantitative comparisons of different bboxes. As shown in Tab. 3, Gen stands for the generation bboxes, while Eva stands for the evaluation bboxes. The two types of bboxes do not significantly affect background preservation in our method, whereas our bboxes perform better than GT bboxes on the foreground metric. More detailed comparisons can be found in *Supp.*

SECR. To verify the effectiveness of SECR, we conduct ablation studies including removing SECR from (1) source branch (w/o source), (2) target branch (w/o target), (3) both (w/o source & target). The visualization results are illustrated in columns 3 to 5 of Fig. 7. Although all methods preserve the background well, they show reduced foreground

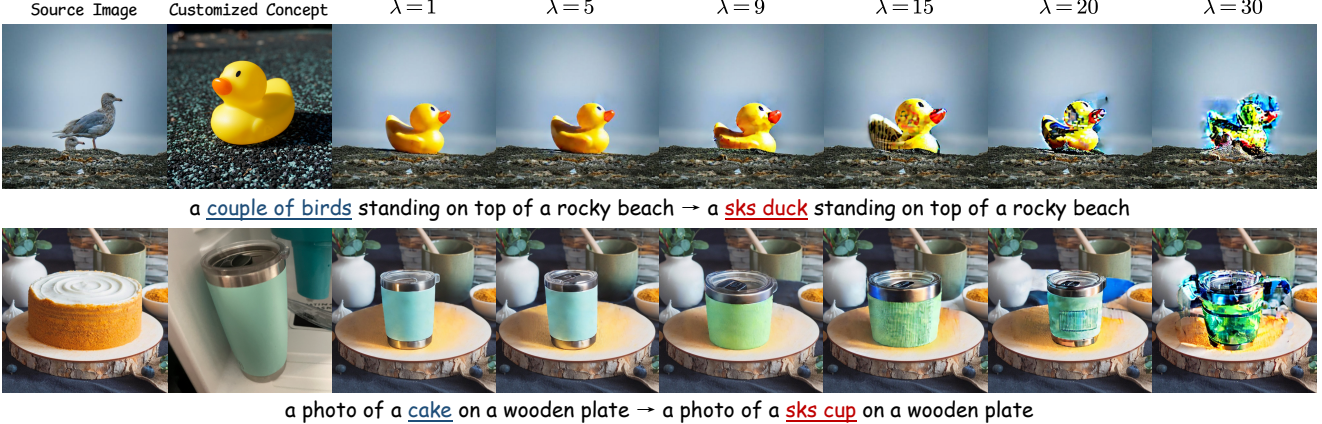


Fig 8. Qualitative results of different SSGU factor λ . Excessively high λ can lead to a decline in foreground consistency.

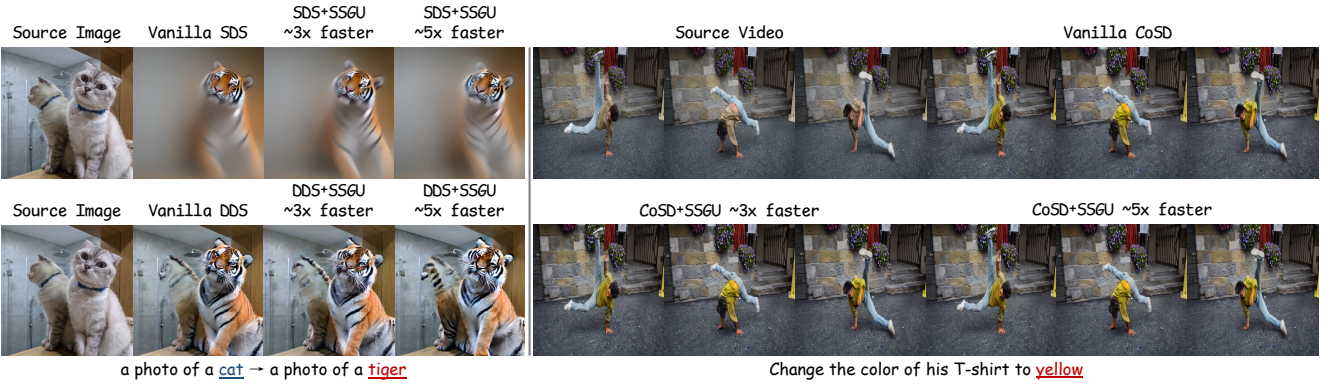


Fig 9. Qualitative results of extending our SSGU to other score distillation based methods.

Table 3. Quantitative ablation results of different bboxes.

Gen	Eva	CLIP-I ↑	PSNR ↑	LPIPS ↓	MSE ↓	SSIM ↑	CLIP-T ↑
Ours	GT	75.00	27.39	47.68	27.87	86.58	25.74
GT	GT	75.79	31.46	32.61	13.51	87.62	25.53
Ours	Ours	77.72	31.64	31.17	13.28	88.21	25.74

fidelity. Additionally, we perform a quantitative analysis of their foreground consistency and prompt consistency. The results presented in Tab. 4 indicate that our full method exhibits superior performance.

Table 4. Quantitative ablation results of SECR.

Method	CLIP-I ↑	CLIP-T ↑
w/o source	73.70	25.47
w/o target	73.40	25.52
w/o source&target	72.42	25.21
Ours	75.00	25.74

SSGU. To verify the effectiveness of our proposed SSGU, we first visualize the images generated under different

SSGU factors. As shown in Fig. 8, $\lambda = 1$ indicates that SSGU is not used. When $\lambda \leq 9$, the SSGU can preserve foreground and background consistency well while improving the efficiency of our method. As λ increases, the images exhibit more artifacts due to excessive neglect of gradients. Therefore, identifying an optimal SSGU factor λ is crucial. We further conduct a detailed quantitative analysis of different λ values on foreground consistency and efficiency (see complete results in *Supp.*), as illustrated in Fig. 11, where the x -axis represents different λ values and the y -axis represents the respective metric outcomes. When SSGU is not used, our method achieves the best swapping consistency but the lowest efficiency. As λ increases, our SSGU sacrifices certain swapping consistency but significantly improves efficiency. To balance consistency and efficiency, we ultimately select $\lambda = 5$ for our final model.

4.6. Applications of INSTANTSWAP

Multi-concept swapping. Our INSTANTSWAP can be easily extended to facilitate multi-concept swaps by sequentially performing multiple single-concept swaps. As shown in the left of Fig. 10, our method can swap each concept



Fig 10. INSTANTSWAP can be extended to other tasks such as: *Left*: Multi-Concept Swapping. *Middle*: Human Face Swapping. *Right*: Concept Insertion and Removal.

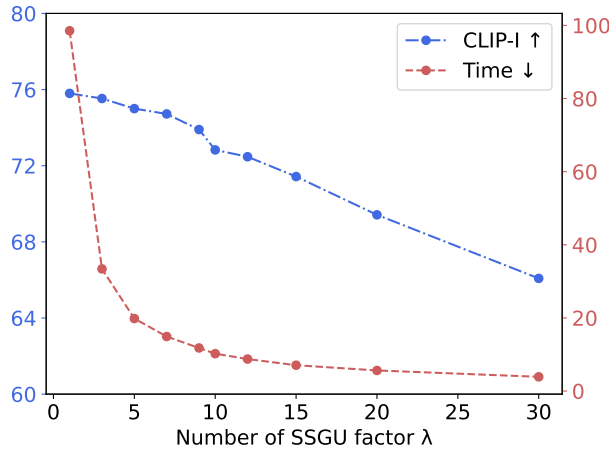


Fig 11. Quantitative results on the ablation study of the SSGU factor λ .

within the image with both foreground and background consistency.

Human face swapping. INSTANTSWAP demonstrates exceptional capabilities in human face swapping. As shown in the middle of Fig. 10, with customized face models from CivitAI [5], users can seamlessly replace the face in a source image with a customized target face.

Concept insertion and removal. In addition to concept swapping, our method also supports concept insertion and removal. For concept insertion, we employ the same procedure as concept swapping. For concept removal, we adjust the target prompt and the target semantic input p_t of SECR to a null prompt. The results in the right of Fig. 10 further demonstrate the versatility of our method.

Table 5. Quantitative results of SSGU extension.

Method	w/o SSGU	w/ SSGU $\lambda = 3$	w/ SSGU $\lambda = 5$
SDS	40.37s	14.12s	8.62s
DDS	66.89s	22.65s	13.90s
CoSD	344.76s	128.97s	79.15s

Accelerating other methods. SSGU can be transferred to other score distillation based methods to enhance their efficiency. We select three representative methods: SDS [39], DDS [19] for image editing, and CoSD [25] for video edit-

ing. As shown in Fig. 9, combining these methods with SSGU can significantly improve their efficiency while almost not altering the generation quality. We further conduct a quantitative analysis to assess the transferability of the proposed SSGU, as presented in Tab. 5.

5. Conclusion

This paper introduces INSTANTSWAP, a novel framework for precise and efficient customized concept swap. Our BGM and SECR collaborate to maintain both background and foreground consistency. Furthermore, we propose the SSGU to eliminate redundant computation and improve efficiency. Finally, we introduce *ConSwapBench*, a comprehensive benchmark dataset for customized concept swapping. The impressive performance of INSTANTSWAP demonstrates its effectiveness. We hope our INSTANTSWAP can inspire future research, particularly in efficiently managing concept swapping with obvious shape variance. Future work could focus on (1) extending image-based customized concept swapping to the video domain; (2) enhancing the images of target concepts with low-level methods [9, 16, 17]; and (3) achieving more lightweight and precise concept swapping.

References

- [1] Tim Brooks, Aleksander Holynski, and Alexei A Efros. Instructpix2pix: Learning to follow image editing instructions. In *Proceedings of the IEEE/CVF Conference on Computer Vision and Pattern Recognition*, pages 18392–18402, 2023. 3
- [2] Mingdeng Cao, Xintao Wang, Zhongang Qi, Ying Shan, Xiaohu Qie, and Yingqiang Zheng. Masactrl: Tuning-free mutual self-attention control for consistent image synthesis and editing. In *Proceedings of the IEEE/CVF International Conference on Computer Vision*, pages 22560–22570, 2023. 3
- [3] Hangeol Chang, Jinho Chang, and Jong Chul Ye. Ground-a-score: Scaling up the score distillation for multi-attribute editing. *arXiv preprint arXiv:2403.13551*, 2024. 3
- [4] Jooyoung Choi, Yunjey Choi, Yunji Kim, Junho Kim, and Sungroh Yoon. Custom-edit: Text-guided image editing with customized diffusion models. *arXiv preprint arXiv:2305.15779*, 2023. 2, 3
- [5] Civitai. Civitai. <https://civitai.com/>, 2024. 10
- [6] Guillaume Couairon, Jakob Verbeek, Holger Schwenk, and Matthieu Cord. Diffedit: Diffusion-based seman-

tic image editing with mask guidance. *arXiv preprint arXiv:2210.11427*, 2022. 3

[7] Prafulla Dhariwal and Alexander Nichol. Diffusion models beat gans on image synthesis. *Advances in neural information processing systems*, 34:8780–8794, 2021. 1

[8] Wenkai Dong, Song Xue, Xiaoyue Duan, and Shumin Han. Prompt tuning inversion for text-driven image editing using diffusion models. In *Proceedings of the IEEE/CVF International Conference on Computer Vision*, pages 7430–7440, 2023. 3

[9] Chengyu Fang, Chunming He, Fengyang Xiao, Yulun Zhang, Longxiang Tang, Yuelin Zhang, Kai Li, and Xiu Li. Real-world image dehazing with coherence-based pseudo labeling and cooperative unfolding network. In *The Thirty-eighth Annual Conference on Neural Information Processing Systems*, 2024. 10

[10] Rinon Gal, Yuval Alaluf, Yuval Atzmon, Or Patashnik, Amit H Bermano, Gal Chechik, and Daniel Cohen-Or. An image is worth one word: Personalizing text-to-image generation using textual inversion. *arXiv preprint arXiv:2208.01618*, 2022. 3

[11] Zigang Geng, Binxin Yang, Tiansai Hang, Chen Li, Shuyang Gu, Ting Zhang, Jianmin Bao, Zheng Zhang, Houqiang Li, Han Hu, et al. Instructdiffusion: A generalist modeling interface for vision tasks. In *Proceedings of the IEEE/CVF Conference on Computer Vision and Pattern Recognition*, pages 12709–12720, 2024. 3

[12] Ian Goodfellow, Jean Pouget-Abadie, Mehdi Mirza, Bing Xu, David Warde-Farley, Sherjil Ozair, Aaron Courville, and Yoshua Bengio. Generative adversarial networks. *Communications of the ACM*, 63(11):139–144, 2020. 2

[13] Jing Gu, Yilin Wang, Nanxuan Zhao, Tsu-Jui Fu, Wei Xiong, Qing Liu, Zhifei Zhang, He Zhang, Jianming Zhang, HyunJoon Jung, et al. Photoswap: Personalized subject swapping in images. *Advances in Neural Information Processing Systems*, 36, 2024. 2, 3, 8

[14] Jing Gu, Yilin Wang, Nanxuan Zhao, Wei Xiong, Qing Liu, Zhifei Zhang, He Zhang, Jianming Zhang, HyunJoon Jung, and Xin Eric Wang. Swapanything: Enabling arbitrary object swapping in personalized visual editing. *arXiv preprint arXiv:2404.05717*, 2024. 2, 3, 8

[15] Qin Guo and Tianwei Lin. Focus on your instruction: Fine-grained and multi-instruction image editing by attention modulation. In *Proceedings of the IEEE/CVF Conference on Computer Vision and Pattern Recognition*, pages 6986–6996, 2024. 3

[16] Chunming He, Chengyu Fang, Yulun Zhang, Kai Li, Longxiang Tang, Chenyu You, Fengyang Xiao, Zhenhua Guo, and Xiu Li. Reti-diff: Illumination degradation image restoration with retinex-based latent diffusion model. 2023. 10

[17] Chunming He, Yuqi Shen, Chengyu Fang, Fengyang Xiao, Longxiang Tang, Yulun Zhang, Wangmeng Zuo, Zhenhua Guo, and Xiu Li. Diffusion models in low-level vision: A survey. *arXiv preprint arXiv:2406.11138*, 2024. 10

[18] Amir Hertz, Ron Mokady, Jay Tenenbaum, Kfir Aberman, Yael Pritch, and Daniel Cohen-Or. Prompt-to-prompt image editing with cross attention control. *arXiv preprint arXiv:2208.01626*, 2022. 2, 3, 8

[19] Amir Hertz, Kfir Aberman, and Daniel Cohen-Or. Delta denoising score. In *Proceedings of the IEEE/CVF International Conference on Computer Vision*, pages 2328–2337, 2023. 2, 3, 4, 8, 10

[20] Jack Hessel, Ari Holtzman, Maxwell Forbes, Ronan Le Bras, and Yejin Choi. Clipscore: A reference-free evaluation metric for image captioning. *arXiv preprint arXiv:2104.08718*, 2021. 8

[21] Jonathan Ho, Ajay Jain, and Pieter Abbeel. Denoising diffusion probabilistic models. *Advances in neural information processing systems*, 33:6840–6851, 2020. 6

[22] Wenjing Huang, Shikui Tu, and Lei Xu. Pfb-diff: Progressive feature blending diffusion for text-driven image editing. *arXiv preprint arXiv:2306.16894*, 2023. 3

[23] Yuzhou Huang, Liangbin Xie, Xintao Wang, Ziyang Yuan, Xiaodong Cun, Yixiao Ge, Jiantao Zhou, Chao Dong, Rui Huang, Ruimao Zhang, et al. Smartedit: Exploring complex instruction-based image editing with multimodal large language models. In *Proceedings of the IEEE/CVF Conference on Computer Vision and Pattern Recognition*, pages 8362–8371, 2024. 3

[24] Xuan Ju, Ailing Zeng, Yuxuan Bian, Shaoteng Liu, and Qiang Xu. Pnp inversion: Boosting diffusion-based editing with 3 lines of code. In *The Twelfth International Conference on Learning Representations*, 2024. 2, 3, 8

[25] Subin Kim, Kyungmin Lee, June Suk Choi, Jongheon Jeong, Kihyuk Sohn, and Jinwoo Shin. Collaborative score distillation for consistent visual synthesis. *arXiv preprint arXiv:2307.04787*, 2023. 3, 10

[26] Nupur Kumari, Bingliang Zhang, Richard Zhang, Eli Shechtman, and Jun-Yan Zhu. Multi-concept customization of text-to-image diffusion. In *Proceedings of the IEEE/CVF Conference on Computer Vision and Pattern Recognition*, pages 1931–1941, 2023. 2, 3

[27] Pengzhi Li, Qiang Nie, Ying Chen, Xi Jiang, Kai Wu, Yuhuan Lin, Yong Liu, Jinlong Peng, Chengjie Wang, and Feng Zheng. Tuning-free image customization with image and text guidance. *arXiv preprint arXiv:2403.12658*, 2024. 3

[28] Tianle Li, Max Ku, Cong Wei, and Wenhui Chen. Dreamedit: Subject-driven image editing. *arXiv preprint arXiv:2306.12624*, 2023. 2, 3

[29] Bingyan Liu, Chengyu Wang, Tingfeng Cao, Kui Jia, and Jun Huang. Towards understanding cross and self-attention in stable diffusion for text-guided image editing. In *Proceedings of the IEEE/CVF Conference on Computer Vision and Pattern Recognition*, pages 7817–7826, 2024. 4

[30] Yue Ma, Xiaodong Cun, Yingqing He, Chenyang Qi, Xintao Wang, Ying Shan, Xiu Li, and Qifeng Chen. Magic-stick: Controllable video editing via control handle transformations. *arXiv preprint arXiv:2312.03047*, 2023. 3

[31] Yue Ma, Yingqing He, Xiaodong Cun, Xintao Wang, Siran Chen, Xiu Li, and Qifeng Chen. Follow your pose: Pose-guided text-to-video generation using pose-free videos. In *Proceedings of the AAAI Conference on Artificial Intelligence*, pages 4117–4125, 2024. 3

[32] Yue Ma, Yingqing He, Hongfa Wang, Andong Wang, Chenyang Qi, Chengfei Cai, Xiu Li, Zhifeng Li, Heung-Yeung Shum, Wei Liu, et al. Follow-your-click: Open-domain regional image animation via short prompts. *arXiv preprint arXiv:2403.08268*, 2024. 3

[33] Yue Ma, Hongyu Liu, Hongfa Wang, Heng Pan, Yingqing He, Junkun Yuan, Ailing Zeng, Chengfei Cai, Heung-Yeung Shum, Wei Liu, et al. Follow-your-emoji: Fine-controllable and expressive freestyle portrait animation. *arXiv preprint arXiv:2406.01900*, 2024. 3

[34] Daiki Miyake, Akihiro Iohara, Yu Saito, and Toshiyuki Tanaka. Negative-prompt inversion: Fast image inversion for editing with text-guided diffusion models. *arXiv preprint arXiv:2305.16807*, 2023. 3

[35] Ron Mokady, Amir Hertz, Kfir Aberman, Yael Pritch, and Daniel Cohen-Or. Null-text inversion for editing real images using guided diffusion models. In *Proceedings of the IEEE/CVF Conference on Computer Vision and Pattern Recognition*, pages 6038–6047, 2023. 2, 3

[36] Hyelin Nam, Gihyun Kwon, Geon Yeong Park, and Jong Chul Ye. Contrastive denoising score for text-guided latent diffusion image editing. In *Proceedings of the IEEE/CVF Conference on Computer Vision and Pattern Recognition*, pages 9192–9201, 2024. 2, 3, 8

[37] Quang Nguyen, Truong Vu, Anh Tran, and Khoi Nguyen. Dataset diffusion: Diffusion-based synthetic data generation for pixel-level semantic segmentation. *Advances in Neural Information Processing Systems*, 36, 2024. 4

[38] Alex Nichol, Prafulla Dhariwal, Aditya Ramesh, Pranav Shyam, Pamela Mishkin, Bob McGrew, Ilya Sutskever, and Mark Chen. Glide: Towards photorealistic image generation and editing with text-guided diffusion models. *arXiv preprint arXiv:2112.10741*, 2021. 1

[39] Ben Poole, Ajay Jain, Jonathan T Barron, and Ben Mildenhall. Dreamfusion: Text-to-3d using 2d diffusion. *arXiv preprint arXiv:2209.14988*, 2022. 2, 3, 4, 5, 8, 10

[40] Alec Radford, Jong Wook Kim, Chris Hallacy, Aditya Ramesh, Gabriel Goh, Sandhini Agarwal, Girish Sastry, Amanda Askell, Pamela Mishkin, Jack Clark, et al. Learning transferable visual models from natural language supervision. In *International conference on machine learning*, pages 8748–8763. PMLR, 2021. 8

[41] Tianhe Ren, Shilong Liu, Ailing Zeng, Jing Lin, Kunchang Li, He Cao, Jiayu Chen, Xinyu Huang, Yukang Chen, Feng Yan, et al. Grounded sam: Assembling open-world models for diverse visual tasks. *arXiv preprint arXiv:2401.14159*, 2024. 7

[42] Herbert Robbins and Sutton Monro. A stochastic approximation method. *The annals of mathematical statistics*, pages 400–407, 1951. 7

[43] Robin Rombach, Andreas Blattmann, Dominik Lorenz, Patrick Esser, and Björn Ommer. High-resolution image synthesis with latent diffusion models. In *Proceedings of the IEEE/CVF conference on computer vision and pattern recognition*, pages 10684–10695, 2022. 1, 2, 4, 7

[44] Nataniel Ruiz, Yuanzhen Li, Varun Jampani, Yael Pritch, Michael Rubinstein, and Kfir Aberman. Dreambooth: Fine tuning text-to-image diffusion models for subject-driven generation. In *Proceedings of the IEEE/CVF conference on computer vision and pattern recognition*, pages 22500–22510, 2023. 2, 3, 7

[45] Jiaming Song, Chenlin Meng, and Stefano Ermon. Denoising diffusion implicit models. *arXiv preprint arXiv:2010.02502*, 2020. 6

[46] Narek Tumanyan, Michal Geyer, Shai Bagon, and Tali Dekel. Plug-and-play diffusion features for text-driven image-to-image translation. In *Proceedings of the IEEE/CVF Conference on Computer Vision and Pattern Recognition*, pages 1921–1930, 2023. 3

[47] Jiangshan Wang, Yue Ma, Jiayi Guo, Yicheng Xiao, Gao Huang, and Xiu Li. Cove: Unleashing the diffusion feature correspondence for consistent video editing. *arXiv preprint arXiv:2406.08850*, 2024. 3

[48] Zhou Wang, Alan C Bovik, Hamid R Sheikh, and Eero P Simoncelli. Image quality assessment: from error visibility to structural similarity. *IEEE transactions on image processing*, 13(4):600–612, 2004. 8

[49] Binxin Yang, Shuyang Gu, Bo Zhang, Ting Zhang, Xuejin Chen, Xiaoyan Sun, Dong Chen, and Fang Wen. Paint by example: Exemplar-based image editing with diffusion models. In *Proceedings of the IEEE/CVF Conference on Computer Vision and Pattern Recognition*, pages 18381–18391, 2023. 2, 3

[50] Kai Zhang, Lingbo Mo, Wenhui Chen, Huan Sun, and Yu Su. Magicbrush: A manually annotated dataset for instruction-guided image editing. *Advances in Neural Information Processing Systems*, 36, 2024. 3

[51] Richard Zhang, Phillip Isola, Alexei A Efros, Eli Shechtman, and Oliver Wang. The unreasonable effectiveness of deep features as a perceptual metric. In *Proceedings of the IEEE conference on computer vision and pattern recognition*, pages 586–595, 2018. 8

[52] Shiwen Zhang, Shuai Xiao, and Weilin Huang. Forgedit: Text guided image editing via learning and forgetting. *arXiv preprint arXiv:2309.10556*, 2023. 3

[53] Yanbing Zhang, Mengping Yang, Qin Zhou, and Zhe Wang. Attention calibration for disentangled text-to-image personalization. In *Proceedings of the IEEE/CVF Conference on Computer Vision and Pattern Recognition*, pages 4764–4774, 2024. 4

[54] Chenyang Zhu, Kai Li, Yue Ma, Chunming He, and Li Xiu. Multibooth: Towards generating all your concepts in an image from text. *arXiv preprint arXiv:2404.14239*, 2024. 3